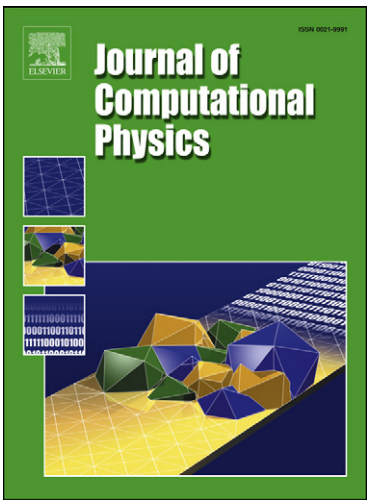

A Wigner Monte Carlo approach to density functional theory

J.M. Sellier, I. Dimov

PII: S0021-9991(14)00252-6
DOI: 10.1016/j.jcp.2014.03.065
Reference: YJCPH 5187

To appear in: *Journal of Computational Physics*

Received date: 23 December 2013
Revised date: 26 March 2014
Accepted date: 28 March 2014

Please cite this article in press as: J.M. Sellier, I. Dimov, A Wigner Monte Carlo approach to density functional theory, *Journal of Computational Physics* (2014), http://dx.doi.org/10.1016/j.jcp.2014.03.065

A Wigner Monte Carlo Approach to Density Functional Theory

J.M. Sellier [a] I. Dimov [a]

[a] *IICT, Bulgarian Academy of Sciences, Acad.G.Bonchev str. 25A, 1113 Sofia, Bulgaria*

Abstract

In order to simulate quantum N-body systems, stationary and time-dependent density functional theories rely on the capacity of calculating the single-electron wavefunctions of a system from which one obtains the total electron density (Kohn-Sham systems). In this paper, we introduce the use of the Wigner Monte Carlo method in ab-initio calculations. This approach allows time-dependent simulations of chemical systems in the presence of reflective and absorbing boundary conditions. It also enables an intuitive comprehension of chemical systems in terms of the Wigner formalism based on the concept of phase-space. Finally, being based on a Monte Carlo method, it scales very well on parallel machines paving the way towards the time-dependent simulation of very complex molecules. A validation is performed by studying the electron distribution of three different systems, a Lithium atom, a Boron atom and a hydrogenic molecule. For the sake of simplicity, we start from initial conditions not too far from equilibrium and show that the systems reach a stationary regime, as expected (despite no restriction is imposed in the choice of the initial conditions). We also show a good agreement with the standard density functional theory for the hydrogenic molecule. These results demonstrate that the combination of the Wigner Monte Carlo method and Kohn-Sham systems provides a reliable computational tool which could, eventually, be applied to more sophisticated problems.

Key words: Density Functional Theory, Wigner equation, Monte Carlo Methods, Kohn-Sham systems, Computational Chemistry

1 Introduction

The simulation of quantum N-body systems is a complex task which requires immense computational resources. It is also an important problem which touches many aspects of our everyday life. Indeed such simulations can explain

complex chemical reactions, assist the design of new materials and enable the development of new technologies, just to mention a few possibilities. Thus it is not surprising that a very early interest has been shown in this direction [1], [2]. For decades now, very big efforts have been made to develop reliable methods and efficient techniques.

Today, in the branch of organic and inorganic computational chemistry, the density functional theory (DFT) can be considered the most popular and used tool. It has shown to be successful in simulating and explaining a plethora of complex quantum systems [3]. DFT relies on our capability of calculating the wave-function of a single-electron Schrödinger equation. Indeed, in this theory the quantum N-body problem is reduced to a system of coupled single-electron equations, known as the Kohn-Sham system. The electron-electron interaction is taken into account by means of a so-called density functional, in both stationary and time-dependent regimes [4], [5]. This simplification allows the simulation of N-body problems in more reasonable computational times. The price to pay consists in the fact that the exact mathematical expression for the density functional is known only for simple cases and further approximations are introduced for more complex systems. Nowadays, one can choose between different functionals among which the most popular in chemistry are the local density approximation (LDA) [4], the generalized gradient approximation [6] and the B3LYP [7].

Despite the approximations introduced, in practical calculations the single-electron Schrödinger equation cannot be solved analytically and sophisticated numerical approaches are required which are based on finite difference or finite element methods. Depending on the complexity of the problem involved, these techniques can have problems in scaling on parallel machines. From this perspective, the Wigner Monte Carlo (WMC) method represents a big advantage. This method is based on the iterative Monte Carlo (MC) method for solving linear equations (both integral and algebraic) [8], as well as non-linear equations [9]. Being a MC technique, it is known to scale very well on parallel machines [10] and, thus, opens the way towards the simulation of complex situations hardly approachable in the context of finite difference or finite element methods. Furthermore, the Wigner equation is a formulation of quantum mechanics in terms of a phase-space and, as such, can represent a more convenient approach [11]. Indeed, it is a more intuitive framework to explain quantum mechanics, totally equivalent to the Schrödinger model, which uses a quasi-distribution function (see, for example, [12] and [13] for the description of hydrogen and closed-shell atoms, and [14] for the description of resonant tunneling diodes). Finally, it is possible to choose different boundary conditions (BCs). For chemical systems, we can apply reflective BCs (equivalent to the closed-box assumption) or absorbing BCs (which are time-irreversible and thus in agreement with the requirements in [15]). The case of injecting BCs is still an open problem [16] but not relevant for the calculations performed in

this work. The Wigner equation has been already applied to study a variety of situations ranging from atomic physics [17], [18] to quantum electronic transport [19], [20], [21] but, to the best of our knowledge, has never been utilized for ab-initio simulations.

The first attempts to simulate quantum phenomena with the Wigner equation were based on finite difference approaches which were affected by numerical problems [22], [15], [23] due to the diffusion term of the Liouville operator. Indeed the Wigner quasi-distribution function is rapidly oscillating in the phase space, especially where quantum interference is dominant. During the last decade several MC methods, which avoid the calculation of the diffusion term, were developed [24], [25], [26], [14], [27]. One of them introduces the concept of signed particles, generated by the Wigner potential, but needs ergodic conditions and is relevant only for stationary problems [27]. Recently, this approach has been generalized to the time-dependent regime [28]. This method exploits the notions of momentum quantization and indistinguishable particles. These concepts entangled with the notions of Newtonian trajectories, particle ensemble, and particle annihilation allow the implementation of time-dependent, full quantum, and multi-dimensional simulations.

In this work, we propose a variant of the standard DFT, where the set of coupled single-electron *Schrödinger* equations in the Kohn-Sham system is substituted by an equivalent set of single-electron *Wigner* equations, which are solved by the WMC method. We validate our proposed approach by applying it to the study of three different quantum systems: a Lithium atom, a Boron atom and an hydrogenic molecule in two different configurations (close and far apart nuclei). Furthermore, in the last system, we perform a comparison with the standard DFT. For these systems one expects that, starting from well educated initial conditions (the only restriction being the Heinsenberg principle not to be violated), the electron densities should eventually tend to a stationary solution of the standard Kohn-Sham system. This is what we observe from our numerical experiments, in excellent (quantitative) agreement with the standard DFT, paving the way towards scalable simulations of complex chemical systems in the Wigner formalism.

2 A Wigner Monte Carlo Approach to DFT

The goal of DFT is the simulation of quantum N-body systems. In the time-dependent framework, the dynamics of such systems is described by the many-body Schrödinger equation:

$$i\hbar\frac{\partial}{\partial t}\Psi = \hat{H}\Psi, \tag{1}$$

where the unknown is the (complex) wave-function $\Psi = \Psi(\mathbf{r}_1, \ldots, \mathbf{r}_N)$, $\mathbf{r}_i = (x_i, y_i, z_i)$ represents the position of the i-th particle, and the functional $\hat{H}$, known as the Hamiltonian of the system, acts on the space of wave-functions and accounts for the various forces involved in the problem:

$$\hat{H} = \left[\sum_{i=1}^{N} \left(-\frac{\hbar^2 \nabla_i^2}{2m_i} \right) - \sum_{i,j=1}^{N} \frac{Z_j e^2}{|\mathbf{r}_i - \mathbf{r}_j|} + \frac{1}{2} \sum_{i \neq j}^{N} \frac{e^2}{|\mathbf{r}_i - \mathbf{r}_j|} \right]. \tag{2}$$

The resolution of (1) represents an incredible mathematical challenge even when approached by numerical techniques. It is worth to mention that attempts in this direction have been made (direct MC minimization techniques [29]) but, up to now, they only allow the calculation of the stationary ground state.

In 1926 a first attempt to simplify the problem (1), altough in the stationary case, was done by introducing an approximate method to find the electronic structure in terms of a one-electron ground-state density $\rho(\mathbf{r})$, [1], [2]. The Thomas-Fermi theory, as it is known today, introduces too many oversimplifications to be of any pratical use but it represents a foundational result for the development of DFT. Later on, Slater combined the ideas of Thomas and Fermi with the Hartree's orbital method [30], [31], introducing for the first time a local exchange potential. Then the Hohenberg-Kohn theorem proved that, in principle, an exact method using the one-electron ground-state density $\rho(\mathbf{r})$ [32] can be depicted and the Kohn-Sham system was introduced from the homogeneous quantum electron gas theory [4]. The time-dependent counterpart of the Hohenberg-Kohn theorem was introduced in 1984 which is known as the Runge-Gross theorem [5]. One should note that this theorem guarantees the validity of the time-dependent Kohn-Sham system only for the calculations of the ground-state properties. Nothing is proved about the excited states. In this work, we anyway use the time-dependent Kohn-Sham system as a first preliminary step to introduce the use of the single-electron Wigner MC method in ab-initio calculations (further developments will follow in the next future to improve this approach).

Despite its limitations, the time-dependent Kohn-Sham system greatly reduces the difficulties involved in (1) and allows practical and useful (but not yet chemical) simulations of quantum N-body systems. Indeed, we now deal with a set of N one-electron Schrödinger equations coupled to each other by means of an artificial density functional $v_{\text{eff}}(\mathbf{r})$ which is local [3]. One should note that the locality of this functional introduces severe restrictions to the time-dependent simulations of strongly correlated electron systems. Anyway, for the above reasons, we use it as preliminary introduction of the Wigner MC method in ab-initio calculations.

The time-dependent Kohn-Sham system consists of the following set of equa-

tions ($i = 1 \dots N$)

$$i\hbar \frac{\partial \Phi_i}{\partial t}(\mathbf{r}, t) = \left(-\frac{\hbar^2 \nabla^2}{2m_i} + v_{\text{eff}}(\mathbf{r}) \right) \Phi_i(\mathbf{r}, t) \tag{3}$$

from which the one-electron density can be calculated in the following way:

$$\rho(\mathbf{r}) = \sum_i |\Phi_i(\mathbf{r})|^2, \tag{4}$$

where the sum is performed over the states below the Fermi energy. The N-body effects are included in the effective potential $v_{\text{eff}} = v_{\text{eff}}(\mathbf{r})$ which can be expressed in terms of an external potential (usually representing the potential due to the nuclei of a molecule), the Hartree potential and an exchange-correlation potential

$$v_{\text{eff}}(\mathbf{r}) = v_{\text{ext}}(\mathbf{r}) + e^2 \int d\mathbf{r}' \frac{\rho(\mathbf{r}')}{|\mathbf{r} - \mathbf{r}'|} + v_{\text{xc}}[\rho](\mathbf{r}). \tag{5}$$

Finally, one should note that there is no unique way to express the density functional v_{xc}. Many choices are available (e.g. [4], [6] and [7]). In any case, given a functional, it is possible to solve the set of equations (3) from which one obtains the one-electron density $\rho(\mathbf{r})$.

The Wigner formulation of quantum mechanics offers a description of the electron state in terms of a quasi-distribution function $f_w = f_w(\mathbf{r}, \mathbf{p}, t)$, where $\mathbf{r}$ is the position and $\mathbf{p}$ the momentum. The Wigner function f_w is related to the Schrödinger wave-function $\Psi(\mathbf{r}, t)$ via the following Wigner-Weyl transform:

$$f_w(\mathbf{r}, \mathbf{p}, t) = \frac{1}{i\hbar 2\pi} \int d\mathbf{r}' e^{-i\frac{\mathbf{p}\cdot\mathbf{r}'}{\hbar}} \Psi(\mathbf{r} + \frac{\mathbf{r}'}{2}, t) \Psi^*(\mathbf{r} - \frac{\mathbf{r}'}{2}, t). \tag{6}$$

By applying it to the time-dependent Schrödinger equation, one obtains the time-dependent evolution of the quasi-distribution function, known as the Wigner equation [11]

$$\frac{\partial f_w}{\partial t} + \frac{\mathbf{p}}{m} \cdot \nabla_{\mathbf{r}} f_w = Q[f_w], \tag{7}$$

where the functional $Q[f_w]$ is defined over the space of pseudo-distribution functions:

$$Q[f_w](\mathbf{r}, \mathbf{p}, t) = \int d\mathbf{p}' V_w(\mathbf{r}, \mathbf{p} - \mathbf{p}', t) f_w(\mathbf{r}, \mathbf{p}', t). \tag{8}$$

The function $V_w = V_w(\mathbf{r}, \mathbf{p}, t)$ is known as the Wigner potential and reads

$$V_w(\mathbf{r}, \mathbf{p}, t) = \frac{1}{i\hbar^2 (2\pi)^3} \int d\mathbf{r}' e^{-i\frac{\mathbf{p}\cdot\mathbf{r}'}{\hbar}} \Big(V(\mathbf{r} + \frac{\mathbf{r}'}{2}, t) - V(\mathbf{r} - \frac{\mathbf{r}'}{2}, t) \Big), \tag{9}$$

where the function $V = V(\mathbf{r}, t)$ is the potential acting over the spatial domain and may vary in time.

It is possible to reformulate this model by exploiting a semi-discrete phase-space [28]. Indeed, by introducing a cut-off length $\mathbf{L}_C = (L_C^x, L_C^y, L_C^z)$, a discrete Fourier transform can be applied in (9), and the space of momenta can be expressed in terms of multiples of the finite quantity $\Delta\mathbf{p} = \frac{\hbar\pi}{\mathbf{L}_C}$. Thus, a momentum vector $\mathbf{p}$ can now be described as a triplet of integers $\mathbf{M} = (M_x, M_y, M_z)$, where $\mathbf{p} = \mathbf{M}\Delta\mathbf{p} = (M_x\Delta p_x, M_y\Delta p_y, M_z\Delta p_z)$. In the phase-space $(\mathbf{r}, \mathbf{M})$, the semi-discrete Wigner equation reads

$$\frac{\partial f_w}{\partial t}(\mathbf{r}, \mathbf{M}, t) + \frac{\mathbf{M}\Delta\mathbf{p}}{m} \cdot \nabla_{\mathbf{r}} f_w(\mathbf{r}, \mathbf{M}, t) = \sum_{\mathbf{N}=-\infty}^{+\infty} V_w(\mathbf{r}, (\mathbf{M} - \mathbf{N})) f_w(\mathbf{r}, \mathbf{N}, t), \tag{10}$$

where the Wigner potential is reformulated accordingly

$$V_w(\mathbf{r}, \mathbf{M}, t) = \frac{1}{i\hbar^2 \mathbf{L}_C} \int_{-\mathbf{L}_C/2}^{+\mathbf{L}_C/2} d\mathbf{r}' e^{-i2\frac{\mathbf{M}\Delta\mathbf{p}\cdot\mathbf{r}'}{\hbar}} \left(V(\mathbf{r} + \mathbf{r}', t) - V(\mathbf{r} - \mathbf{r}', t)\right).$$

We can now reformulate the semi-discrete Wigner equation (10) in an adjoint integral form having a solution which can be expressed in terms of a series. In particular, the expection value of a macroscopic physical quantity $A = A(\mathbf{r}, \mathbf{p})$ can be written as the following series

$$\langle A \rangle = \int_0^\infty dt' \int d\mathbf{r}_i \sum_{\mathbf{M}'=-\infty}^{\infty} f_w^0(\mathbf{r}_i, \mathbf{M}') e^{-\int_0^{t'} \gamma(\mathbf{r}_i(y))dy} g(\mathbf{r}_i(t'), \mathbf{M}', t'), \tag{11}$$

where $f_w^0 = f_w^0(\mathbf{r}, \mathbf{M})$ represents the initial conditions, the function $g = g(\mathbf{r}, \mathbf{M}, t)$ is the solution of the adjoint equation containing the quantity $A = A(\mathbf{r}, \mathbf{p})$, and the function $\gamma = \gamma(\mathbf{r})$ is defined as

$$\gamma(\mathbf{r}) = \sum_{\mathbf{M}=-\infty}^{+\infty} V_w^+(\mathbf{r}, \mathbf{M}), \tag{12}$$

with V_w^+ the positive part of V_w [28].

In order to depict a MC method for the resolution of (10), we report the first two terms of the series and give a physical interpretation. The zeroth term reads:

$$\langle A\rangle_0(\tau) = \int_0^\infty dt' \int d\mathbf{r}_i \sum_{\mathbf{M}'=-\infty}^{\infty} f_w^0(\mathbf{r}_i, \mathbf{M}')$$
$$e^{-\int_0^{t'} \gamma(\mathbf{r}_i(y))dy} A(\mathbf{r}_i(t'), \mathbf{M}')\delta(t'-\tau) \tag{13}$$

From a MC mathematical perspective, the integrand can be considered as a product of conditional probabilities. Indeed, assuming that f_w^0 is normalized, one can generate random points $(\mathbf{r}_i, \mathbf{M}')$ at a given initial time. This can be interpreted as the initialization of particle trajectories $\mathbf{r}_i(y)$ and the exponent of the integrand can be seen as the probability for a particle to remain in its trajectory where the rate is given by the function $\gamma(\mathbf{r})$. A *out-of-trajectory time* (less than τ) can be generated randomly and the probability acts as a filter to the particles: if a particle remains in its initial trajectory until time τ, it contributes to $< A >_0 (\tau)$ with the value $f_w^0(\mathbf{r}_i, \mathbf{M}')A(\mathbf{r}_i(\tau), \mathbf{M}')$. At that point, if N particles remain in the trajectory, $< A >_0 (\tau)$ is estimated by using their initial mean value. Otherwise, if the particle does not stay in its initial trajectory, it does not contribute to $< A >_0 (\tau)$ but to the term $< A >_1 (\tau)$:

$$\langle A\rangle_1(\tau) = \int_0^\infty dt' \int d\mathbf{r}_i \sum_{\mathbf{M}'=-\infty}^{\infty} f_w^0(\mathbf{r}_i, \mathbf{M}')$$
$$\left\{\gamma(\mathbf{r}_i(t'))e^{-\int_0^{t'} \gamma(\mathbf{r}_i(y))dy}\right\} \times \theta_D(\mathbf{r}_1)$$
$$\int_{t'}^\infty dt \sum_{\mathbf{M}=-\infty}^{\infty} \left\{\frac{\Gamma(\mathbf{r}_1, \mathbf{M}, \mathbf{M}')}{\gamma(\mathbf{r}_i(t'))}\right\}$$
$$\left\{e^{-\int_{t'}^{t} \gamma(\mathbf{r}_1(y))dy}\right\} A((\mathbf{r}_1(t), \mathbf{M}, t)\delta(t-\tau), \tag{14}$$

where

$$\begin{aligned}\Gamma(\mathbf{r}, \mathbf{M}, \mathbf{M}') = & V_w^+(\mathbf{r}, \mathbf{M}-\mathbf{M}') \\ & - V_w^+(\mathbf{r}, -(\mathbf{M}-\mathbf{M}')) \\ & + \gamma(\mathbf{r})\delta_{\mathbf{M},\mathbf{M}'}.\end{aligned} \tag{15}$$

This time a particle is initialized at $(\mathbf{r}_i, \mathbf{M}', 0)$ and follows the trajectory until time t' (which is the out-of-trajectory time given by the probability density in the first curly brackets). It is easy to see that the exponent is the probability to stay in the initial trajectory until time t', while $\gamma(\mathbf{r}_i(t'))dt'$ is the probability to leave the trajectory in the interval $[t', t'+dt']$. The particle is now in the phase-space position $(\mathbf{r}_1 = \mathbf{r}_i(t'), \mathbf{M}', t')$ and the evolution continues as long as the particle remains in the simulation domain. Otherwise the domain indicator $\theta_D = \theta_D(\mathbf{r})$ changes the value from 1 to 0 and the contribution is zero. The term in the next curly bracket can be interpreted as a source of momentum variation from $\mathbf{M}'$ to $\mathbf{M}$ (locally in space at point $\mathbf{r}_1$ and time t').

Thus, at moment t' the particle initializes the trajectory $(\mathbf{r}_1, \mathbf{M})$ and, with the probability given by the exponent in the last curly brackets, remains over the trajectory until time τ is reached: t is set to τ by the δ function provided that $t' < \tau$, otherwise the contribution is zero. In the same way, a physical interpretation of the other terms of the series can be given.

From the previous observations, a MC approach for the semi-discrete Wigner equation can now be depicted (see [8], [9] for all details). By considering the quantity $\gamma = \gamma(\mathbf{r})$ in (12) as a normalization factor, the expression (15) describes the generation process of two particles, with a positive and a negative sign respectively, and the surviving initial particle with its sign due to the δ function. More specifically, an initial particle with sign s and momentum $\mathbf{N}$ generates, with a rate $V^+(\mathbf{L})$, two primary particles with signs s, $-s$ and momenta $\mathbf{N}' = \mathbf{N} + \mathbf{L}$, $\mathbf{N}' = \mathbf{N} - \mathbf{L}$, and continues its free flight evolution until a given time T. The created pair, in turn, generates new pairs, etc., and the number of particles increases exponentially. By noting that particles are indistinguishable and that two particles in the same spatial cell with the same momentum $\mathbf{M}$ and opposite signs do not contribute to the Wigner distribution function, an annihilation technique can be implemented to reduce the number of particles during the simulation [28]. The time-dependent evolution of the Wigner quasi-distribution happens only by creation and annihilation of particles which replace the acceleration due to Newtonian forces [28].

By applying the Wigner-Weyl transform (6) to every Schrödinger equation of the set (3), where $V(\mathbf{r}) = v_{\text{eff}}(\mathbf{r})$, it is possible to obtain a new time-dependent Kohn-Sham system expressed in terms of the corresponding N Wigner equations

$$\frac{\partial f_w^i}{\partial t} + \frac{\mathbf{p}}{m} \cdot \nabla_{\mathbf{r}} f_w^i = Q[f_w^i], \tag{16}$$

where the Wigner potential is expressed in terms of an effective potential

$$V_w(\mathbf{r}, \mathbf{p}, t) = \frac{1}{i\hbar^2 (2\pi)^3} \int d\mathbf{r}' e^{-i\frac{\mathbf{p}\cdot\mathbf{r}'}{\hbar}} \Big(v_{\text{eff}}(\mathbf{r} + \frac{\mathbf{r}'}{2}, t) - v_{\text{eff}}(\mathbf{r} - \frac{\mathbf{r}'}{2}, t) \Big). \tag{17}$$

Given an adequate effective potential $v_{\text{eff}}(\mathbf{r})$ which, in turn, depends on the choice of the exchange-correlation functional, the quantum N-body problem now consists of solving the set of coupled equations (16). This system, of course, being based on the same assumptions, is affected by the same problems of standard DFT. The choice of the exchange-correlation potential is not unique and difficult to select, there is no guarantee that the excited states are correct, etc. This approach, if applied to any computational quantum problem, will essentially give the same answers given by the standard DFT. Nevertheless, two important advantages must be underlined in this new model. First, the Wigner formalism is based on the concept of a quasi-distribution function and, as such, can give a much more intuitive representation of the simulated

system. For example, one can discuss the system in terms of single-electron distribution functions and visualize the time-dependent energy distribution which can give profound insights about the dynamics involved. Second, the WMC method, based on the Iterative MC method, is known to be highly scalable outperforming other numerical approaches (the parallelization scheme is trivial) [10]. This opens the way towards simulations of very complex structures.

3 Numerical Experiments

In this section, we present four numerical experiments to validate our proposed method. For all simulations, we utilize the modified time-dependent Kohn-Sham system (16) based on the WMC method. In particular, the first two experiments consist of calculating the stationary configuration of electrons for Lithium and Boron atoms starting from non-stationary initial conditions. These are two important initial experiments since we test the capability of the method to stay in a stationary regime. These are non-trivial experiments since one should remind that the WMC method is based on Newtonian particles constantly moving in free-field trajectories. Reaching a stationary regime and keeping it for a long simulation time is a clear indication of the robustness and reliability of the method. We first simulate the Lithium atom, considered to be a relatively simple case since all orbitals are expected to have a spherical symmetry. Then, we proceed with a Boron atom where this symmetry is not valid anymore for the 2p orbital. Numerically speaking, this represents a more difficult situation to handle. The last two experiments consist of a system constituted of two hydrogen atoms (two fixed positive nuclei and two electrons) and we focus on two different configurations. In the first one the two nuclei are far apart, in the second one they are relatively closer (distance comparable to 1 Angstrom). Eventually both systems evolve towards a stationary regime and, in particular, the apperance of a chemical bond is observable in the second case. Finally, we compare the WMC-DFT solutions with the standard DFT. A good (quantitative) agreement is reached.

For the sake of simplicity, in all experiments the nuclei are modeled as non-screened Coulombic charges. In order to avoid singularities in the numerical treatment of the nuclei, we introduce the following modified potential: [33]:

$$V_i(\mathbf{r}) = \frac{q}{4\pi\epsilon_0 \left((\mathbf{r} - \mathbf{r}_i)^2 + \frac{1}{2}a_0^2 \right)^{\frac{1}{2}}}, \tag{18}$$

where a_0 is the Bohr radius $a_0 = \frac{4\pi\epsilon_0\hbar^2}{me^2}$ (about 0.0529nm) and $\mathbf{r}_i$ is the position of the center of the i-th nucleus. One should note that the choice of this modified Coulombic potential does not represent a restriction for the method.

Indeed one can use any other available mathematical model for nuclei, such as pseudo-potential models, etc. For all experiments, the initial conditions for the Wigner quasi-distribution functions are represented by non-stationary states which are directly proportional in space to the electron density of a hydrogenic state and Gaussian in energy (around a specified energy E_0). For example, for a Lithium atom (2 electrons in 1s state and 1 electron in 2s state), the initial conditions for the 3 electrons are:

$$f_w^{1s}(\mathbf{r},\mathbf{p},0) = A_{1s} e^{\frac{-\left(\frac{p^2}{2m}-E_0\right)}{\sigma_E^2}} e^{-\frac{|\mathbf{r}-\mathbf{r}_i|}{a_0}} \tag{19}$$

(two times) and

$$f_w^{2s}(\mathbf{r},\mathbf{p},0) = A_{2s} e^{\frac{-\left(\frac{p^2}{2m}-E_0\right)}{\sigma_E^2}} e^{-\frac{|\mathbf{r}-\mathbf{r}_i|}{a_0}} \left(1-\frac{|\mathbf{r}-\mathbf{r}_i|}{a_0}\right), \tag{20}$$

where A_{1s} and A_{2s} are normalization constants (the density corresponding to every Wigner quasi-distribution is normalized to unity, i.e. one electron per equation) and σ_E is the dispersion in energy. Again for the sake of simplicity, we choose the following (LDA) exchange-correlation functional taken from [32] (in atomic units):

$$v_{\mathrm{xc}}[\rho](\mathbf{r}) = -\frac{1}{\pi}\left[3\pi^2\rho(\mathbf{r})\right]^{\frac{1}{3}}. \tag{21}$$

One should note that our method is not limited to the choice of any particular exchange-correlation functional. Indeed other (more advanced and reliable) expressions for $v_{\mathrm{xc}}[\rho]$ are available and can be utilized when necessary.

Finally in the last two experiments, involving an hydrogenic molecule, we perform a comparison with the standard DFT. The benchmark system used is the standard time-dependent Kohn-Sham system for two interacting electrons

$$\begin{aligned} i\hbar\frac{\partial\Phi_1}{\partial t}(\mathbf{r},t) &= \left(-\frac{\hbar^2\nabla^2}{2m} + v_{\mathrm{eff}}(\mathbf{r})\right)\Phi_1(\mathbf{r},t) \\ i\hbar\frac{\partial\Phi_2}{\partial t}(\mathbf{r},t) &= \left(-\frac{\hbar^2\nabla^2}{2m} + v_{\mathrm{eff}}(\mathbf{r})\right)\Phi_2(\mathbf{r},t), \end{aligned} \tag{22}$$

where the effective potential v_{eff} is given by (5), v_{xc} is the LDA functional in (21), and the nuclei potentials are expressed by (18). This allows a fair comparison since we use the same exchange-correlation functional and potential model for the nuclei. The method to simulate each of the equations in (22) is based on the implicit in time finite difference scheme proposed in [34].

The Lithium atom. A Lithium atom consists of one nucleus with charge $+3e$ and 3 electrons with negative charge $-e$, interacting with the nucleus and each

other. The system is started from a non-stationary state. Two electrons have initial conditions (19) and one electron have initial conditions (20). The system is evolved in time until a stationary solution is reached. The results of this experiment are reported in Fig.1, Fig.2, Fig.3 and Fig.4. In particular, Fig.1 shows the potential generated by the nucleus and Fig.2 shows the corresponding $\gamma(\mathbf{r})$ function. It is clear from this last figure how the dynamics of the wave packet is affected in proximity of the nucleus. Indeed a zero node can be observed in the position of the nucleus. In other words, no couple of particles is generated in that area. Finally, Fig.3 and Fig.4 show the electron densities corresponding to time equal to 50 attoseconds, for the 1s and 2s states respectively. The system has eventually relaxed toward a stationary state and do not evolve anymore (despite the WMC method is based on continuously evolving Newtonian particles). This is a first indication of the robustness of the method.

The Boron atom. A Boron atom represents a relatively more complex situation since one of his orbitals (2p) does not have spherical symmetry. It consists of one nucleus with charge $+5e$ and 5 electrons with charge $-e$. The system is started from non-stationary initial conditions consisting of two electrons in (19), two electrons in (20) and one electron in the following conditions (density directly proportional to a 2p state):

$$f_w^{2p}(\mathbf{r},\mathbf{k},0) = A_{2p} e^{\frac{-\left(\frac{\hbar^2 k^2}{2m} - E_0\right)}{\sigma_E^2}} e^{-\frac{|\mathbf{r}-\mathbf{r}_i|}{a_0}} (\mathbf{r}-\mathbf{r}_i)^2 . \tag{23}$$

The whole system is evolved until the stationary regime is reached. The results are reported in Fig.5, Fig.6, Fig.7 and Fig.8. In particular, Fig.5 shows the $\gamma(\mathbf{r})$ function at 50 attoseconds corresponding to the nucleus and the electrons. Fig.6, Fig.7 and Fig.8 show the electron densities corresponding to time equal to 50 attoseconds, for the 1s, 2s and 2p states respectively. Even in this numerical experiment, the system converges to a stationary regime as expected. In particular, the 2p orbital remains stationary in time. This is a further indication of the robustness of the method.

Two distant hydrogenic atoms. Two hydrogenic atoms, far apart from each other, create a superposition of two Coulombic potentials in which two electrons interact with each other. The results of this experiment are reported in Fig.9, Fig.11, Fig.13, Fig.15 and Fig.17. In particular, Fig.17 also shows a comparison with the standard DFT method. The initial electron density is shown in Fig.13 while the potential is shown in Fig. 9. The corresponding function $\gamma(\mathbf{r})$ is depicted in Fig.11. Three nodes are clearly visible where no particle is created. These points correspond to the geometric center between the two nuclei and their positions. The system is evolved in time until 50 attoseconds and a stationary solution is already reached at about 4 attoseconds.

The electron density at 50 attoseconds is shown in Fig.15. It is possible to see how the solution is basically tending towards a couple of non-interacting s-shape orbitals which is qualitatively in accordance with the expectation that the system should reach stationary regime if reasonable initial conditions are imposed (in our case not too far from equilibrium). Finally, the cuts for the various densities at 50 attoseconds are shown in Fig.17 along with a comparison with standard DFT results obtained from the system (22). From this plot, it is clear that the two single-electron densities are essentially s-shape non-interacting orbitals. Furthermore, the solution for the total density is (quantitatively) in agreement with the standard DFT. Indeed, the resemblance is striking especially because the methods used for the WMC-DFT and the standard DFT are very different (MC vs. finite differences).

Two close hydrogenic atoms. Two hydrogenic atoms are relatively close to each other (compared to the previous experiment) and two electrons are evolved in the resulting superposition of the nuclei Coulombic potentials. The electron-electron interactions are taken into account by means of the LDA exchange-correlation term (21). In this experiment, these interactions are expected to be important due to the proximity of the nuclei. The system is evolved in time until 50 attoseconds and a stationary solution is already reached at about 5 attoseconds. The results of this experiment are reported in Fig.10, Fig.12, Fig.14, Fig.16 and Fig.18. Fig.14 shows the initial electron density in the total potential of Fig.10. The corresponding $\gamma(\mathbf{r})$ function is depicted in Fig.12. This time one observes only one hole corresponding to the center between the two nuclei and the dynamics is more pronounced in proximity of the two nuclei. This is due to the fact that now interactions are more pronounced. The corresponding electron density is shown in Fig.16. A bond is formed between the two atoms, indeed part of the electron density is spread in the area between the two nuclei. This is clearly shown in Fig.18 where the two single electron densities (dotted curves) and the total density ($o-$ curve) are reported along with the total density obtained from the standard DFT (22) ($.-$ curve). The single-electron densities peaks are centered around one of the two nuclei and spread towards the other nucleus. When combined to form the total density, one observes a chemical bond forming between the two hydrogenic atoms (continuous curve). This is in (qualitative) agreement with our expectations. Furthermore, even for this experiment involving stronger electron-electron interactions, the solution for the total density is (quantitatively) in agreement with the standard DFT. Even in this case, the resemblance is striking showing that our proposed WMC-DFT is reliable and gives reasonable results.

4 Software and Hardware

The results presented in this section have been obtained using the HPC cluster deployed at the Institute of Information and Communication Technologies (IICT) of the Bulgarian Academy of Sciences. This cluster consists of two racks which contain HP Cluster Platform Express 7000 enclosures with 36 blades BL 280c with dual Intel Xeon X5560 @ 2.8Ghz (total 576 cores), 24GB RAM per blade. There are 8 storage and management controlling nodes 8 HP DL 380 G6 with dual Intel X5560 @ 2.8Ghz and 32GB RAM. All these servers are interconnected via non-blocking DDR Infiniband interconnect at 20Gbps line speed. The theoretical peak performance is 3.23Tflops.

The simulator used to obtain the results presented in this paper is a modified version of Archimedes, the GNU package for the simulation of carrier transport in semiconductor devices [35]. This code was first released in 2005, and, since then, users have been able to download the source code under the GNU Public License (GPL). Many features have been introduced in this package. In this particular project, our aim is to develop a full quantum simulator. The code is entirely developed in C and optimized to get the best performance from the hardware. The results of the new version will be posted on the nano-archimedes website (see [36]).

5 Conclusions

In this work, we introduced a novel approach to DFT based on the WMC method. The standard time-dependent Kohn-Sham system (3), exploiting single-electron Schrödinger equations, is modified by applying the Wigner-Weyl transform (6) to every equation such that an equivalent set of coupled Wigner equations is obtained (16) [11]. The new model comes with the very same drawbacks that affect the standard DFT, e.g. there is no unique way to choose the exchange-correlation term, the excited states are not guaranteed to be correct, etc. But it has two main advantages over the standard approach which are worth to be mentioned and could, eventually, have important implications. Firstly, it is based on the Wigner formalism which means that a more intuitive picture can be obtained from simulations in terms of a quasi-distribution function defined over the phase-space [12]. Secondly, it exploits a MC method to solve integro-partial differential equations which, in practice, means trivial and extremely efficient scalability [10]. For validation purposes, we applied our new approach to the simulation of a Lithium atom, a Boron atom and a system consisting of two hydrogenic atoms in two different configurations. The aim of the first two experiments is to show that the WMC method can reach a stationary regime and keep the solution in that

state for very long simulation times. This proves that the method is stable and robust. In particular, this is valid even for the Boron atom which has one atom in a non-trivial 2p state. In the last two experiments involving a hydrogenic molecule, we performed a comparison with standard DFT calculations. The two models, despite they are solved by very different numerical methods (MC vs. finite difference), are in very good (quantitative) agreement, showing that our method is reliable in the range of applicability of DFT. These results pave the way towards highly scalable simulations for computationally complex chemical systems.

6 Acknowledgments

This work has been supported by the the project EC AComIn (FP7-REGPOT-2012-2013-1). The authors would also like to thank Prof. G. Vayssilov for his suggestions.

References

[1] E. Fermi. Un metodo statistico per la determinazione di alcune prioprietà dell'atomo. *Rend. Accad. Naz. Lincei*, 6:602—-607, 1927.

[2] L.H. Thomas. The calculation of atomic fields. *Proc. Cambridge Phil. Soc.*, 23:542—-548, 1927.

[3] W. Kohn. Nobel lecture: Electronic structure of matter - wave functions and density functionals. *Rev. of Mod. Phys.*, 71:1253, 1998.

[4] W. Kohn and L.J. Sham. Self-consistent equations including exchange and correlation effects. *Physical Review*, 140, 4A:1133–1138, 1965.

[5] E. Runge and E.K.U. Gross. Density-functional theory for time-dependent systems. *Phys. Rev. Lett.*, 52:997–1000, 1984.

[6] J.P. Perdew. Density-functional approximation for the correlation energy of the inhomogeneous electron gas. *Phys. Rev. B*, 33:8822, 1986.

[7] C. Lee, W. Yang, and R.G. Parr. Development of the Colle-Salvetti correlation-energy formula into a functional of the electron density. *Phys. Rev. B*, 37:785, 1988.

[8] I. Dimov. Monte Carlo algorithms for linear problems. *Pliska (Studia Mathematica Bulgarica)*, 13:57–77, 2000.

[9] I. Dimov and T. Gurov. Monte Carlo algorithm for solving integral equations with polynomial non-linearity. *Pliska (Studia Mathematica Bulgarica)*, 13:117–132, 2000.

[10] I. Dimov. *Monte Carlo Methods for Applied Scientists*. World Scientific, New Jersey, London, 2008.

[11] E. Wigner. On the quantum correction for thermodynamic equilibrium. *Phys. Rev.*, 40:749, 1932.

[12] J.P. Dalh and M. Springborg. Wigner's phase-space function and atomic structure: I. the hydrogen atom ground state. *Molecular Physics*, 47:1001–1019, 1982.

[13] M. Springborg and J.P. Dalh. Wigner's phase-space function and atomic structure: Ii. ground states for closed-shell atoms. *Phys. Rev. A*, 36:1050–1062, 1987.

[14] D. Querlioz and P. Dollfus. *The Wigner Monte Carlo Method for Nanoelectronic Devices - A Particle Description of Quantum Transport and Decoherence*. ISTE-Wiley, 2010.

[15] W. Frensley. Boundary conditions for open quantum systems driven far from equilibrium. *Rev. Mod. Phys.*, 62:745, 1990.

[16] R. Rosati, F. Dolcini, R.C. Iotti, and F. Rossi. Wigner-function formalism applied to semiconductor quantum devices: Failure of the conventional boundary condition scheme. *Phys. Rev. B*, 88:035401, 2013.

[17] B. Vacchini and K. Hornberger. Relaxation dynamics of a quantum brownian particle in an ideal gas. *Eur. Phys. J. Spec. Top.*, 151:59—-72, 2007.

[18] J.J. Halliwell. Two derivations of the master equation of quantum brownian motion. *J. Phys. A, Math. Theor.*, 40:3067—-3080, 2007.

[19] P. Schwaha, D. Querlioz, P. Dollfus, J. Saint-Martin, M. Nedjalkov, and S. Selberherr. Decoherence effects in the wigner function formalism. *J. Comput. Electron*, 12:388—-396, 2013.

[20] D. Querlioz, J. Saint-Martin, and P. Dollfus. Implementation of the wigner-boltzmann transport equation within particle Monte Carlo simulation. *J. Comput. Electron*, 9:224—-231, 2010.

[21] P. Schwaha, M. Nedjalkov, S. Selberherr, and I. Dimov. Phonon-induced decoherence in electron evolution. pages 472–479, 2011.

[22] N. Kluksdahl, W. Potz, U. Ravaioli, and D.K. Ferry. Wigner function study of a double quantum barrier resonant tunnelling diode. *Superlattices and Microstructures*, 3:41–45, 1987.

[23] K.Y. Kim and B. Lee. On the high order numerical calculation schemes for the Wigner transport equation. *Solid-State Electr.*, 43:2243–2245, 1999.

[24] L. Shifren and D.K. Ferry. Particle Monte Carlo simulation of Wigner function tunneling. *Phys. Lett. A*, 285:217–221, 2001.

[25] L. Shifren and D.K. Ferry. A Wigner function based ensemble Monte Carlo approach for accurate incorporation of quantum effects in device simulation. *J. Comp. Electr.*, 1:55–58, 2002.

[26] L. Shifren and D.K. Ferry. Wigner function quantum Monte Carlo. *Physica B*, 314:72–75, 2002.

[27] M. Nedjalkov, H. Kosina, S. Selberherr, Ch. Ringhofer, and D.K. Ferry. Unified particle approach to Wigner-Boltzmann transport in small semiconductor devices. *Phys. Rev. B*, 70:115319, 2004.

[28] M. Nedjalkov, P. Schwaha, S. Selberherr, J.M. Sellier, and D. Vasileska. Wigner quasi-particle attributes: An asymptotic perspective. *Appl. Phys. Lett.*, 102:163113, 2013.

[29] K. Putteneers and F.Brosens. Monte-Carlo implementation of density-functional theory. *Phys. Rev. B*, 86:085115, 2012.

[30] J.C. Slater. A simplification of the Hartree-Fock method. *Phys. Rev.*, 81:385–390, 1951.

[31] D.R. Hartree. The wave mechanics of an atom with a non-coulomb central field. Part I - theory and methods. *Proc. Camb. Phil. Soc.*, 24:89–110, 1928.

[32] P. Hohenberg and W. Kohn. Inhomogeneous electron gas. *Physical Review*, 136, 1964.

[33] R.W. Hockney and J.W. Eastwood. *Computer Simulation using particles*. A. Hilger, 1988.

[34] A. Goldberg and H.M. Schey. Computer-generated motion pictures of one-dimensional quantum-mechanical transmission and reflection phenomena. *American J. of Phys.*, 35:177, 1967.

[35] J.M. Sellier. Gnu archimedes, October 2013.

[36] J.M. Sellier. nano-archimedes, October 2013.

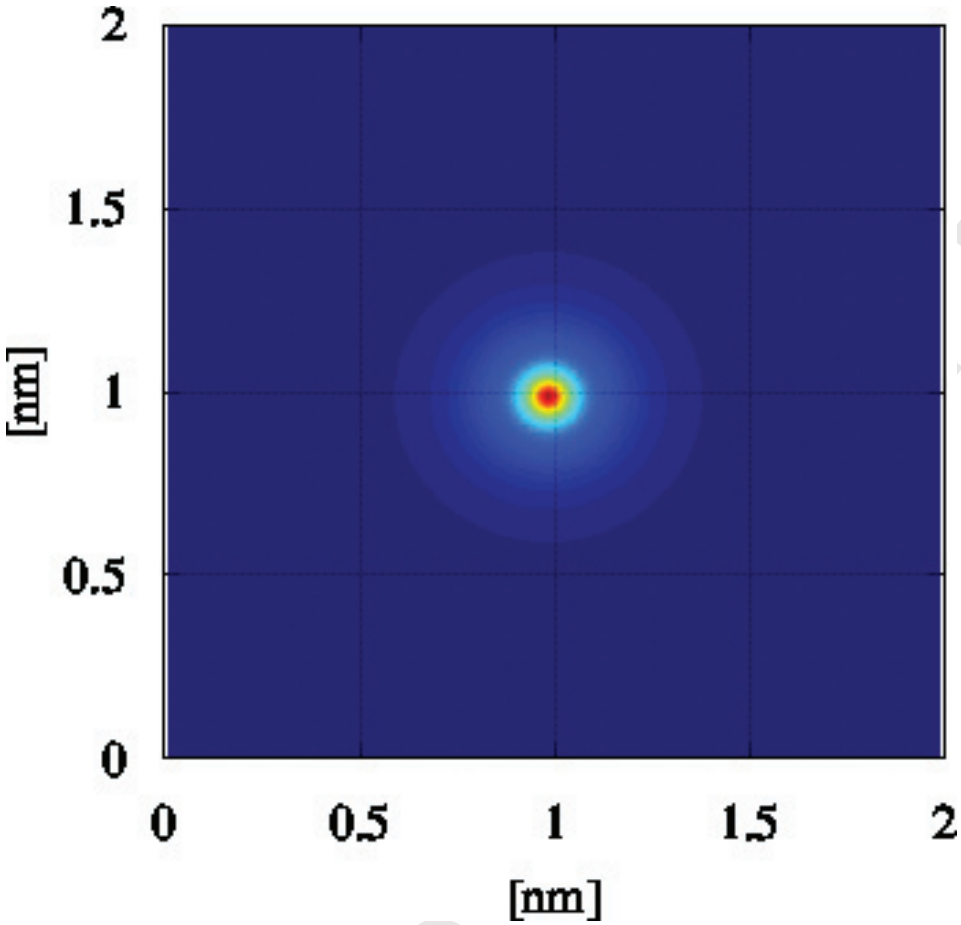

Fig. 1. Nucleus potential created by a Lithium nucleus.

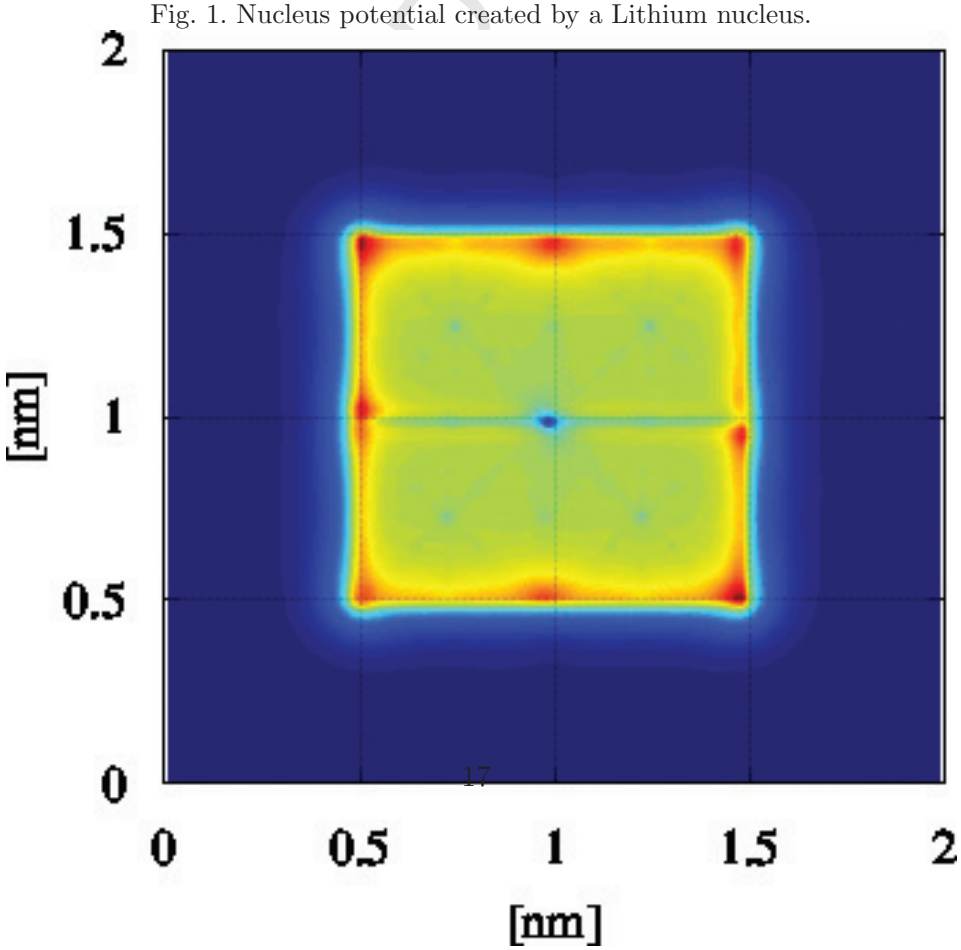

Fig. 2. γ function corresponding to a Lithium atom.

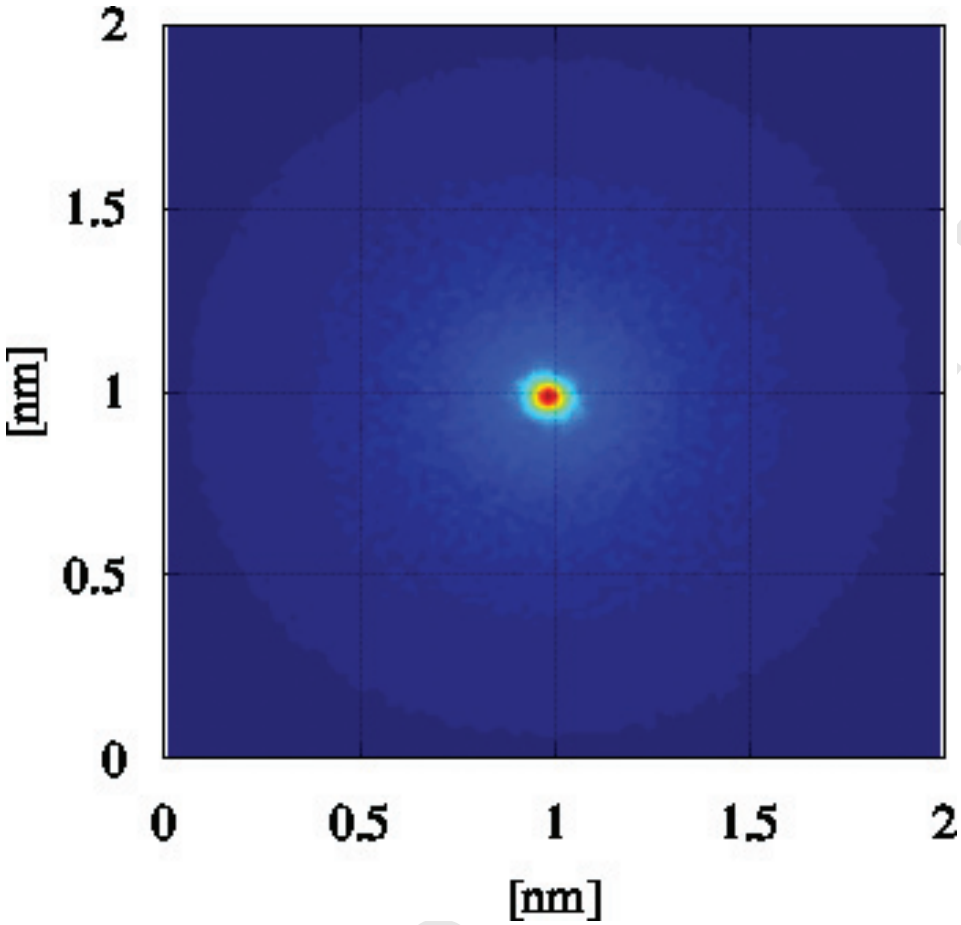

Fig. 3. Density of an electron in Lithium 1s orbital.

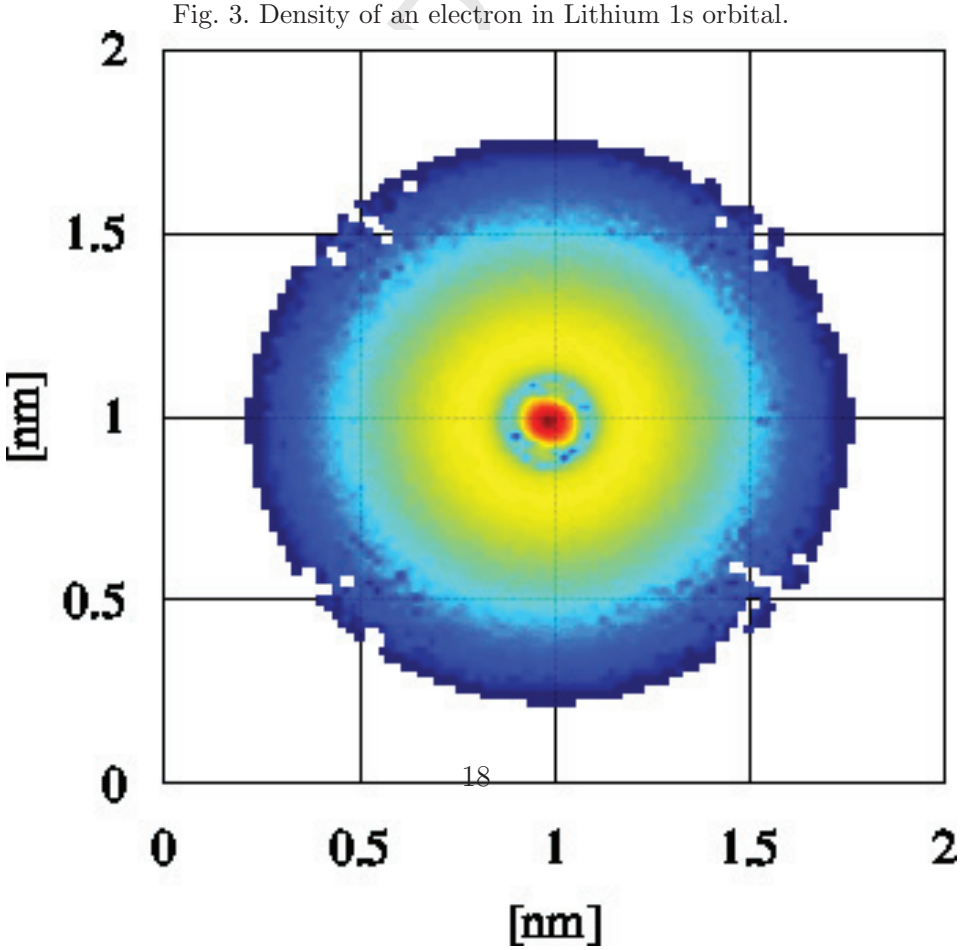

Fig. 4. Density of an electron in Lithium 2s orbital (logarithmic scale).

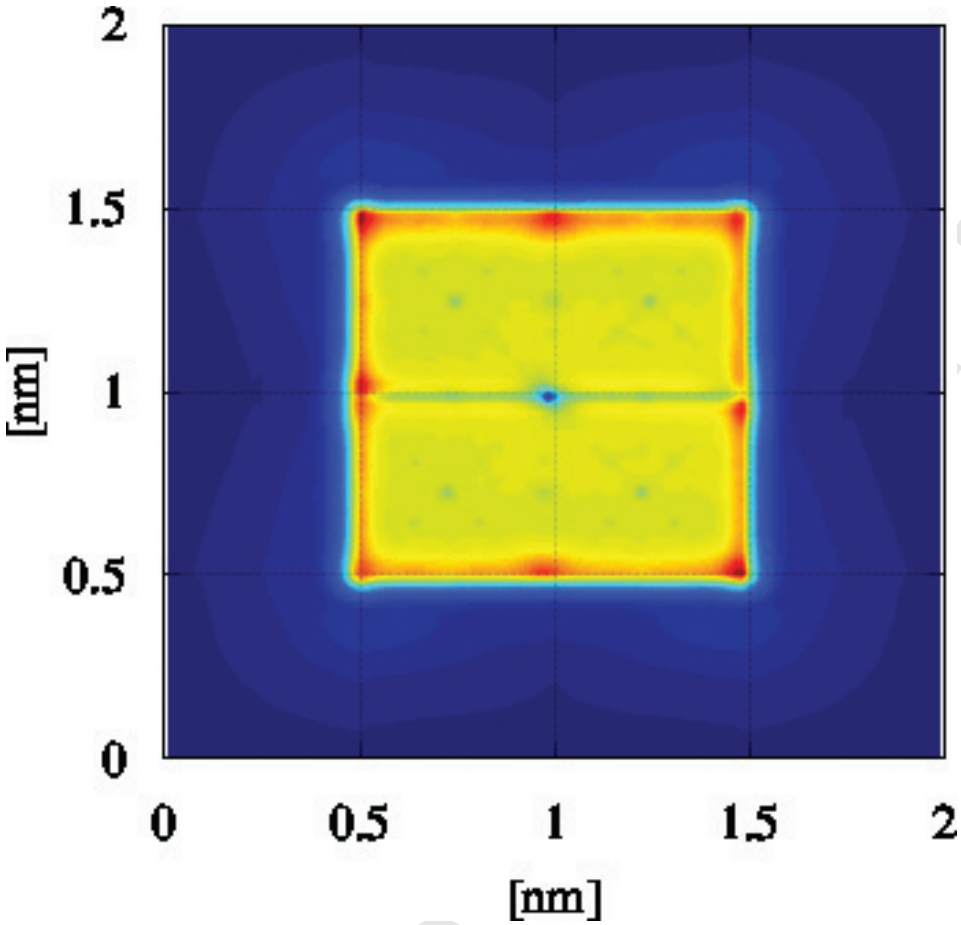

Fig. 5. γ function corresponding to a Boron atom.

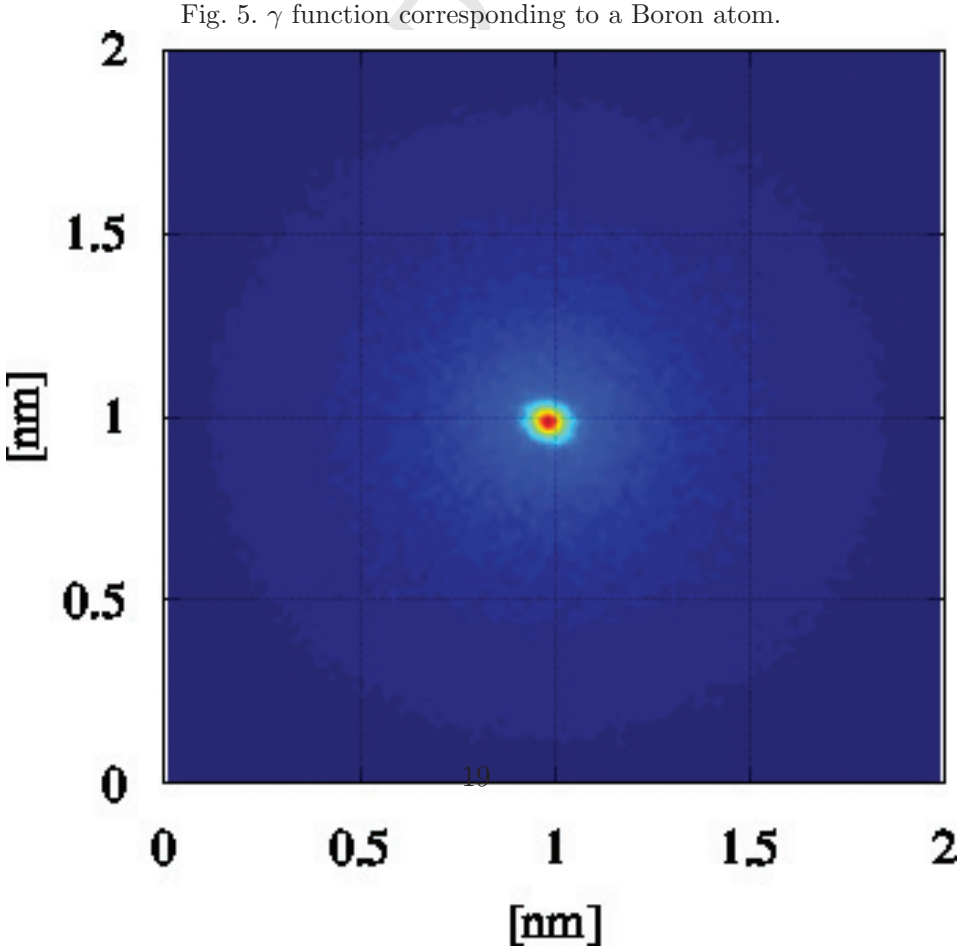

Fig. 6. Density of an electron in Boron 1s orbital.

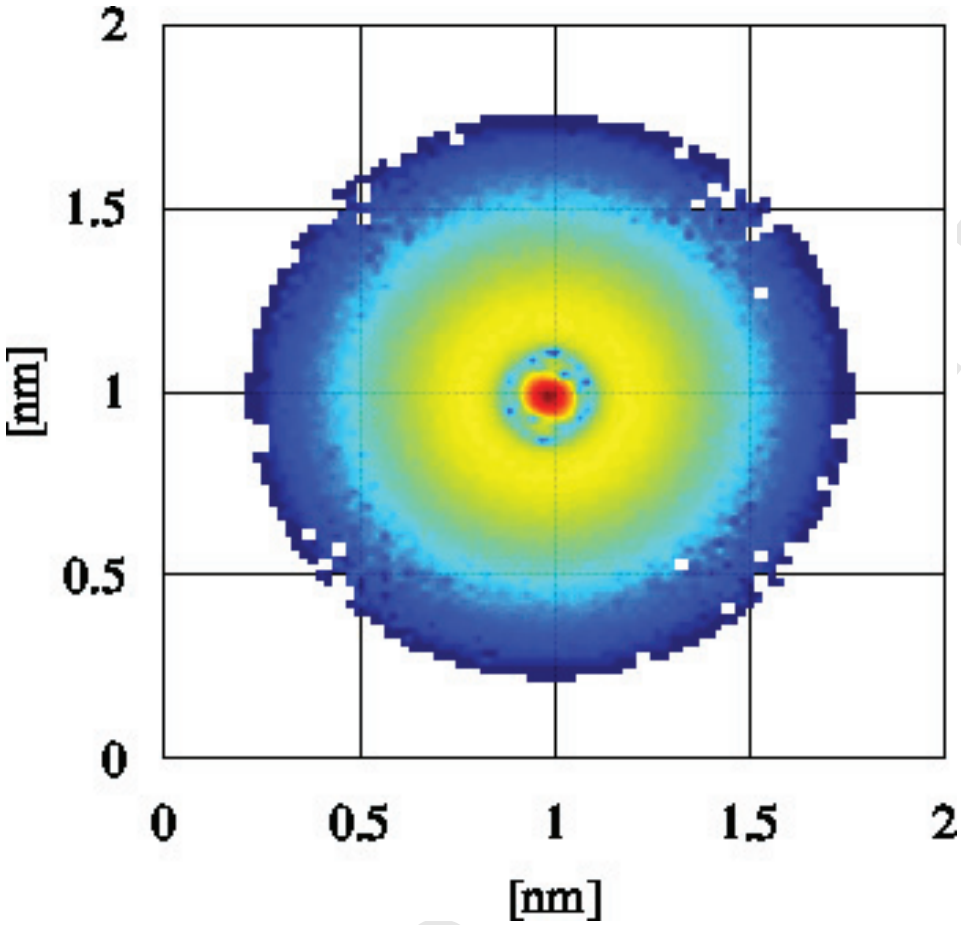

Fig. 7. Density of an electron in Boron 2s orbital (logarithmic scale).

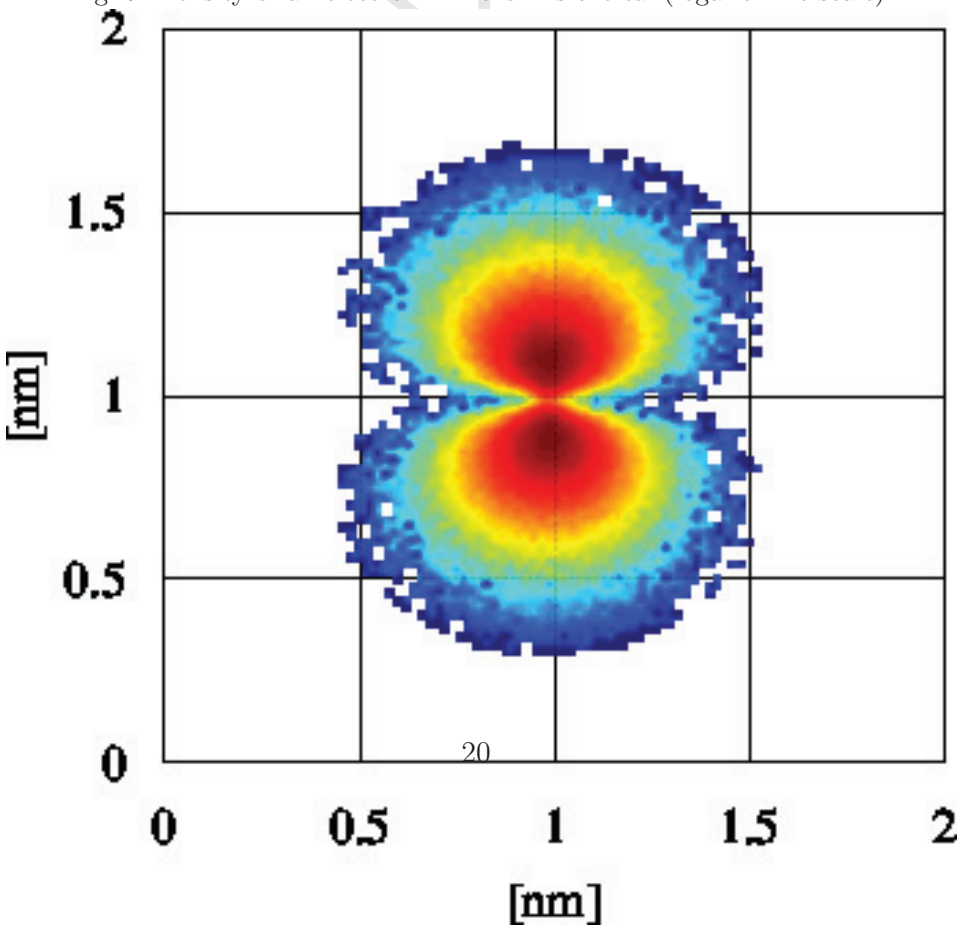

Fig. 8. Density of an electron in Boron 2p orbital (logarithmic scale).

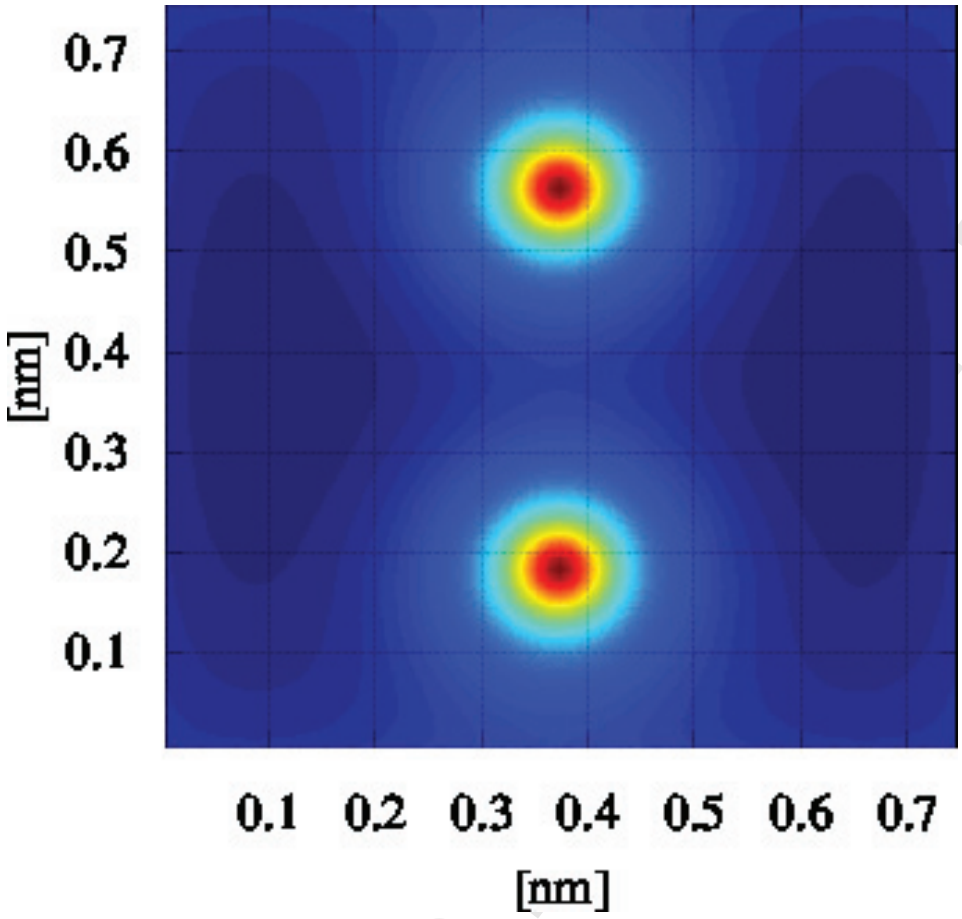

Fig. 9. Nuclei potential created by two distant Hydrogenic atoms.

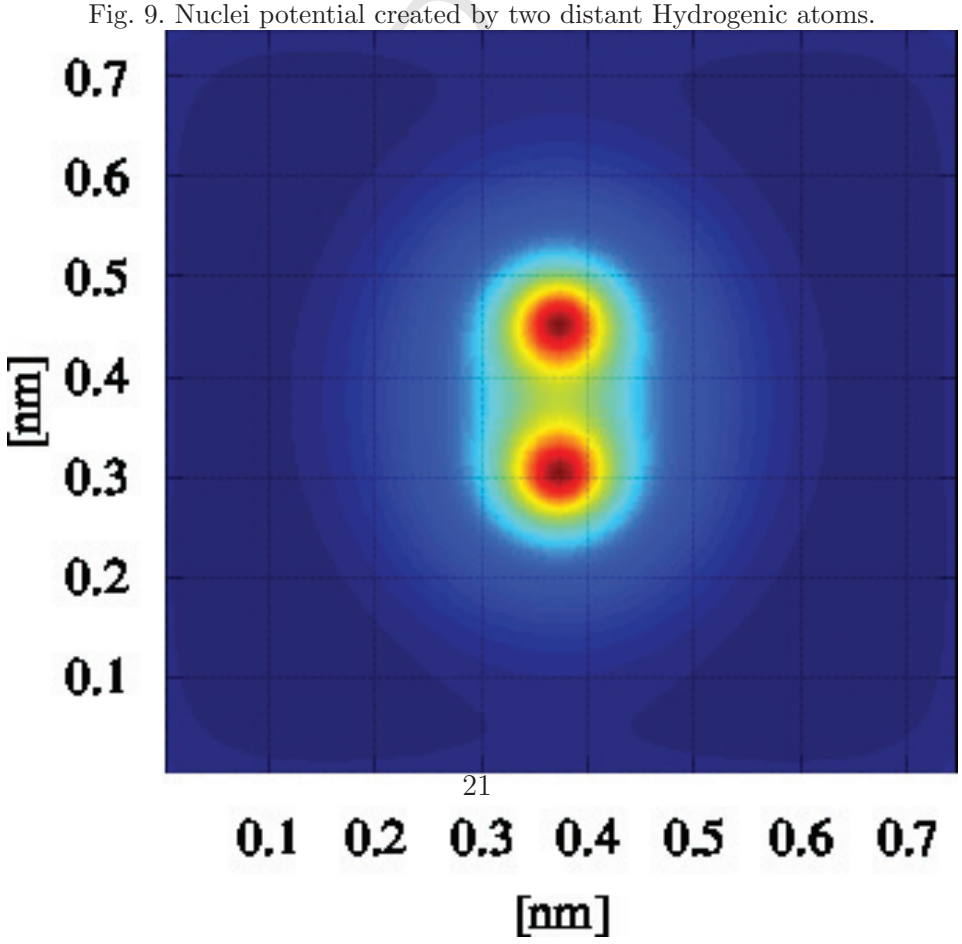

Fig. 10. Nuclei potential created by two close Hydrogenic atoms.

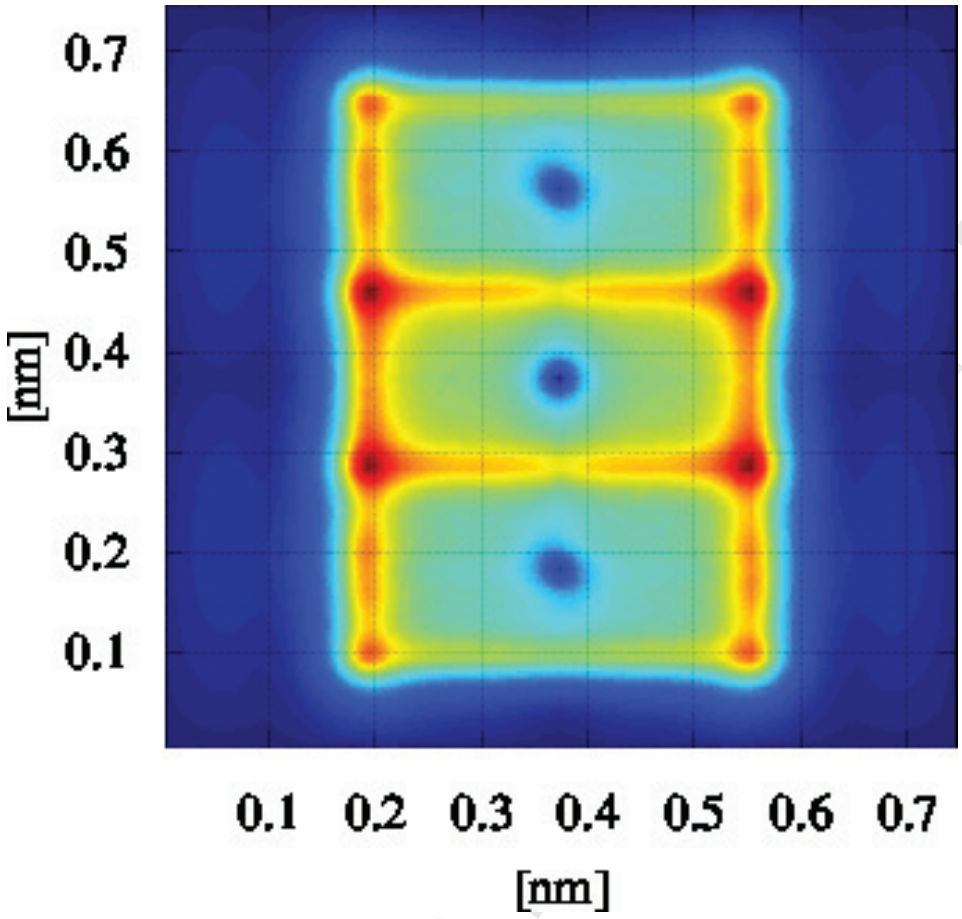

Fig. 11. γ function corresponding to the potential of two distant Hydrogenic nuclei.

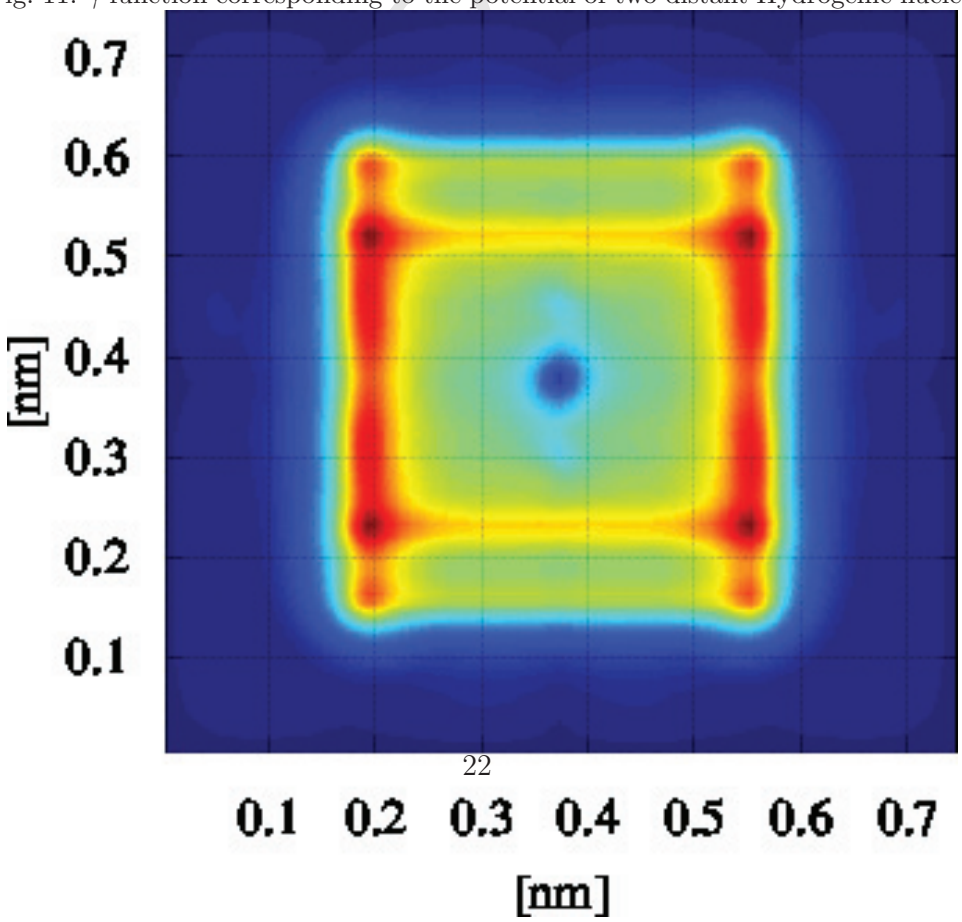

Fig. 12. γ function corresponding to the potential of two close Hydrogenic nuclei.

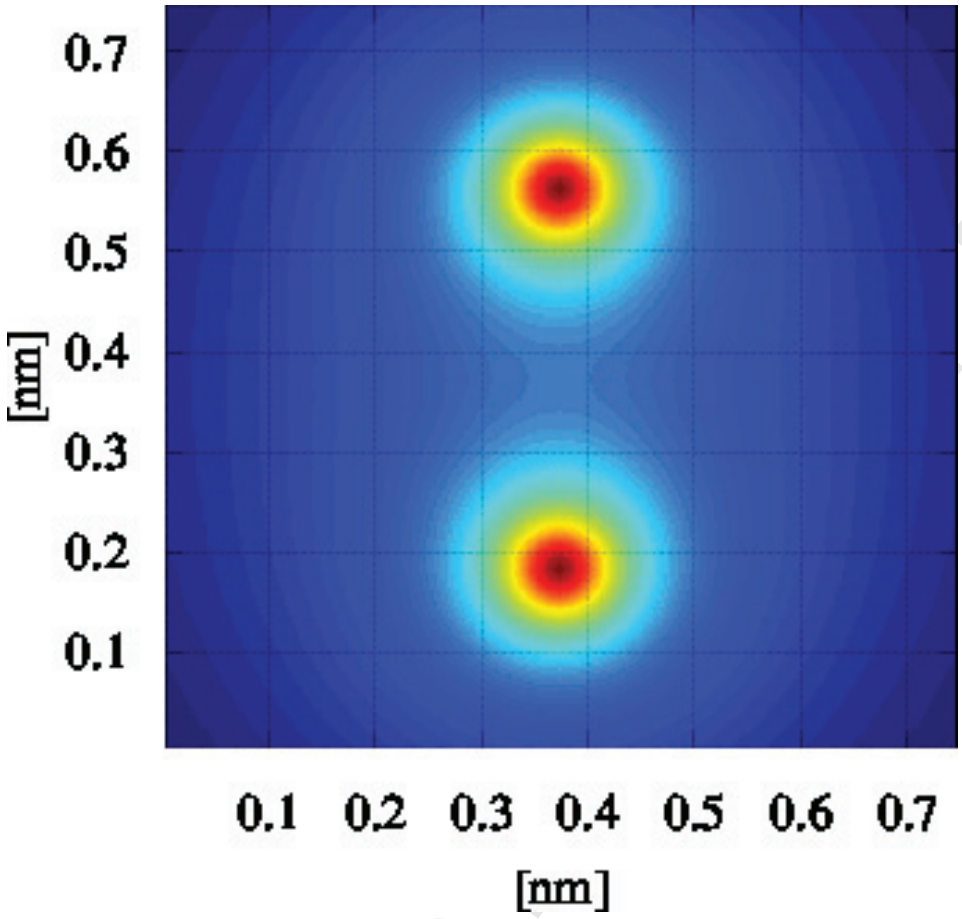

Fig. 13. Initial electron density corresponding to two Gaussian wave packets in proximity of two distant Hydrogenic nuclei.

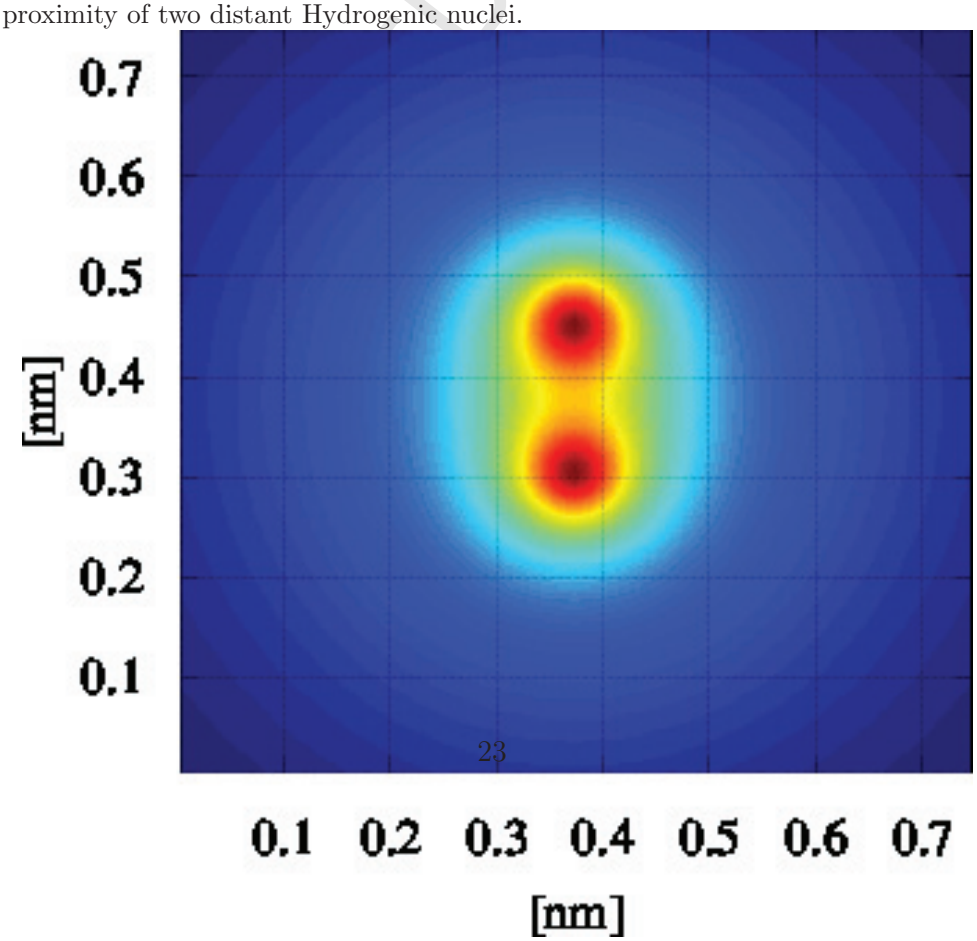

Fig. 14. Initial electron density corresponding to two Gaussian wave packets in

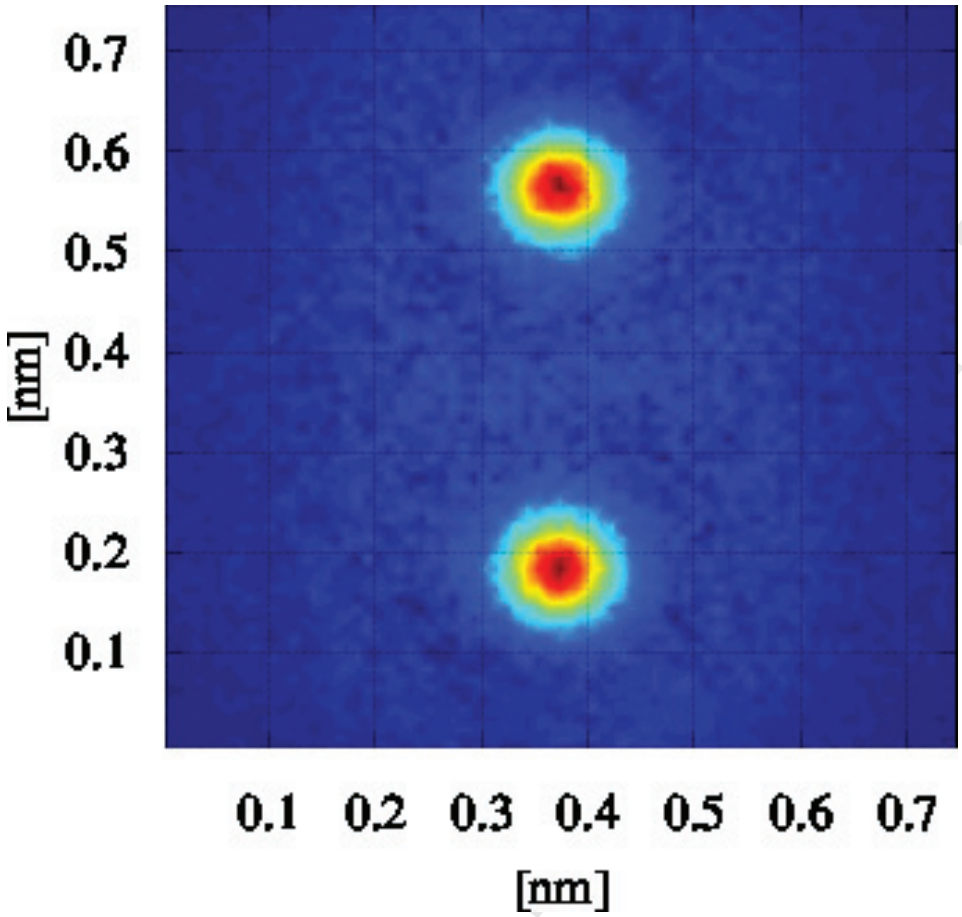

Fig. 15. Electron density at 0.05fs. The two packets tends to two separated s-shape orbitals.

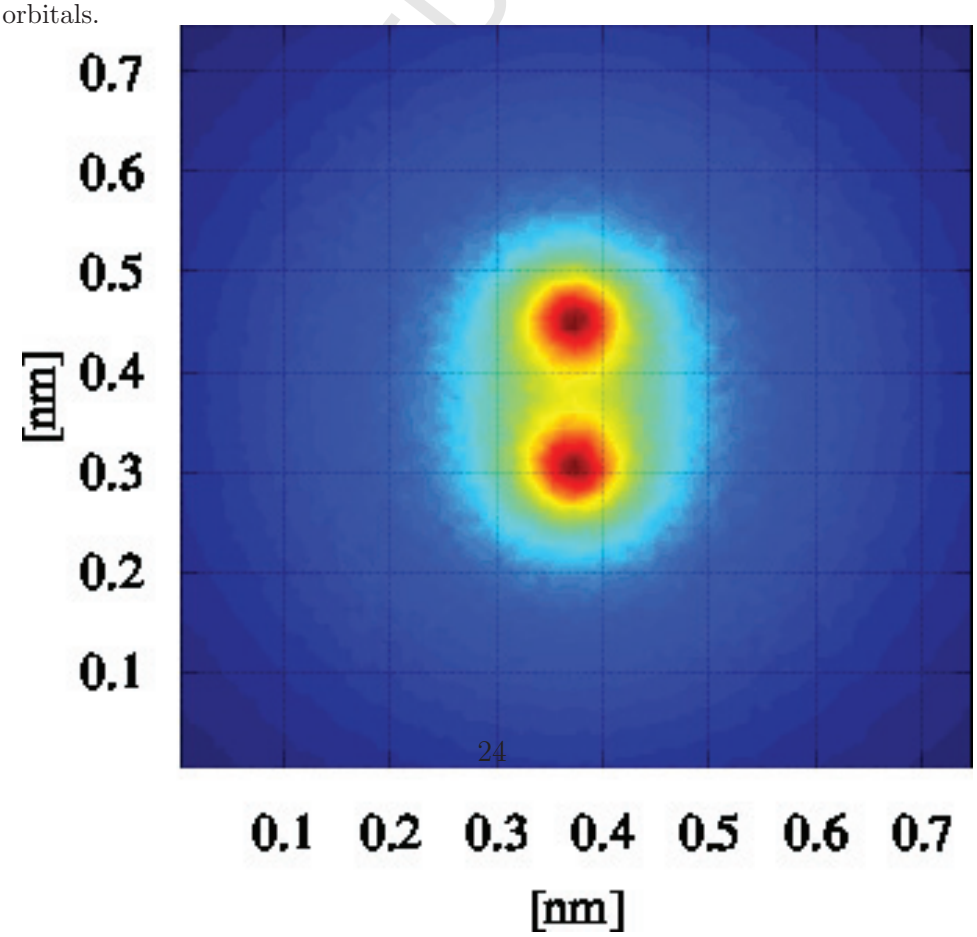

Fig. 16. Electron density at 0.05fs. A bond is formed between the two atoms.

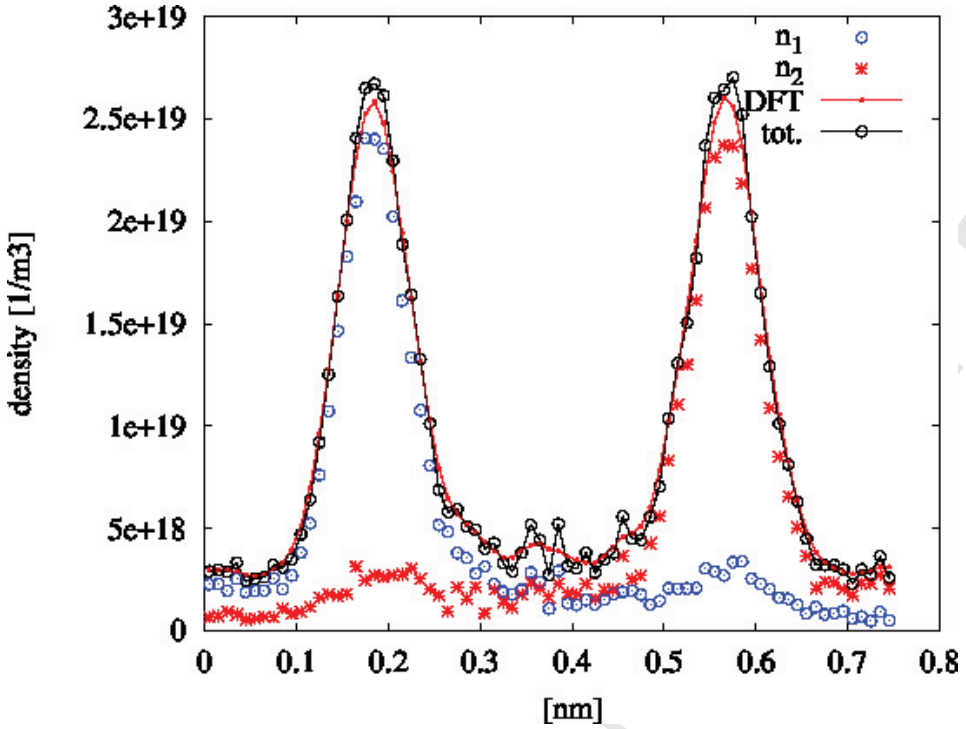

Fig. 17. Cut along the nuclei axis of the electron density at 0.05fs. The two packets (dotted curves) tends to two separated s-shape orbitals. A good agreement is achieved between our proposed model based on WMC, (black) $o-$ line, and the standard DFT, (red) $.-$ line.

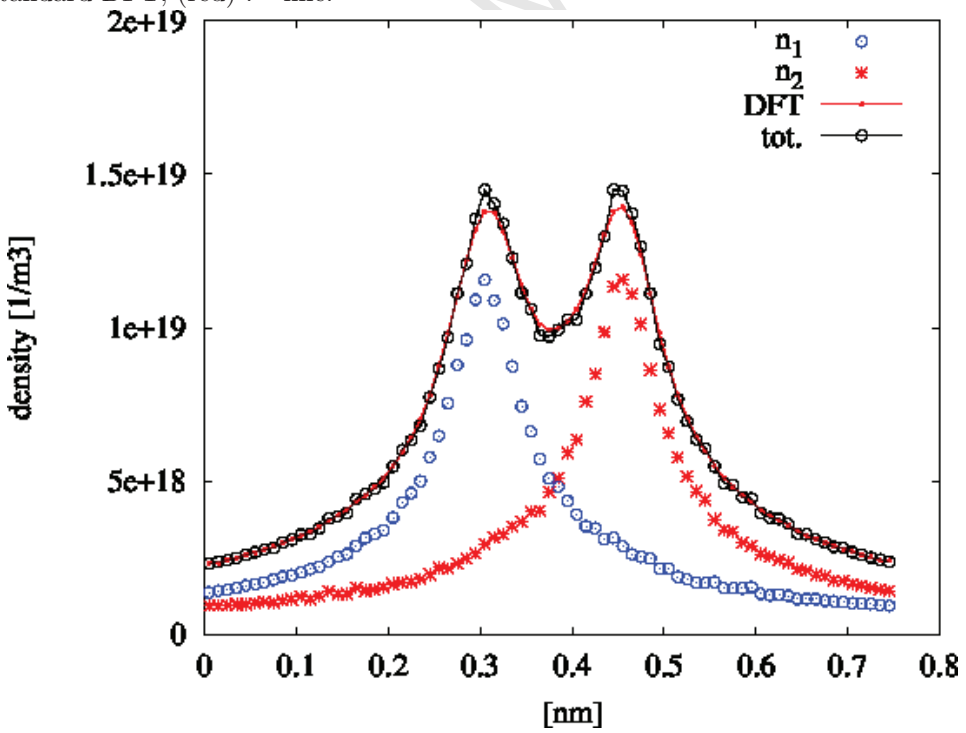

Fig. 18. Cut along the atoms direction of the electron density at 0.05fs. The two packets form a bond between the two Hydrogenic atoms. A good agreement is achieved between our proposed model based on WMC, (black) $o-$ line, and the standard DFT, (red) $.-$ line.